Associated Production of a W Boson and One b Jet

J. Campbell,[1] **R. K. Ellis,**[2] **F. Febres Cordero,**[3] **F. Maltoni,**[4]
L. Reina,[5] **D. Wackeroth**[6], and **S. Willenbrock**[7]

[1]Department of Physics and Astronomy, University of Glasgow
Glasgow G12 8QQ, United Kingdom

[2]Theoretical Physics Department, Fermi National Accelerator Laboratory
P. O. Box 500, Batavia, IL 60510

[3]Department of Physics and Astronomy, UCLA
Los Angeles, CA 90095-1547

[4]Institut de Physique Théorique and
Centre for Particle Physics and Phenomenology (CP3)
Université Catholique de Louvain
Chemin du Cyclotron 2
B-1348 Louvain-la-Neuve, Belgium

[5]Physics Department, Florida State University, Tallahassee, FL 32306-4350

[6]Department of Physics, SUNY at Buffalo, Buffalo, NY 14260-1500

[7]Department of Physics, University of Illinois at Urbana-Champaign
1110 West Green Street, Urbana, IL 61801

Abstract

We calculate the production of a W boson and a single b jet to next-to-leading order in QCD at the Fermilab Tevatron and the CERN Large Hadron Collider. Both exclusive and inclusive cross sections are presented. We separately consider the cross section for jets containing a single b quark and jets containing a $b\bar{b}$ pair. There are a wide variety of processes that contribute, and it is necessary to include them all in order to have a complete description at both colliders.

1 Introduction

Many signals of new physics at hadron colliders involve a weak vector boson (W, Z) plus jets containing heavy quarks (c, b). For example, the top quark was discovered via the signal $W + 4j$, with at least one b jet [1, 2]. More recently, evidence for single top production has been presented via the signal $W + 2j$, with at least one b jet [3, 4, 5, 6]. The Higgs boson could manifest itself via the same signal, from the production process $q\bar{q} \to Wh$, followed by $h \to b\bar{b}$ [7, 8, 9]. The Higgs boson could also appear in the signal $Z + 2j$ with at least one b jet, via $q\bar{q} \to Zh$ [10, 11].

Most calculations of the background processes that give rise to $W, Z + nj$ $(n = 1, 2)$, where one or more jets contain heavy quarks $(Q = c, b)$, have been completed at next-to-leading order (NLO) [12, 13]. There exist NLO calculations of ZQ [14], $ZQ\bar{Q}$ [15, 16], ZQj [17], Wc [18, 19], $Wb\bar{b}$ [20, 21], and Wbj [22]. An obvious omission from this list is Wb, that is, $W + 1j$ with at least one b jet at NLO. It is the goal of this paper to fill in that gap. This NLO calculation can be used to normalize the cross section from a leading-order event generator such as ALPGEN [23] or MadEvent [24].

It may seem surprising that the NLO calculation of Wb has not already been done, given all the other NLO calculations listed above. The reason for this, as we will discuss shortly, is that it is essential to do this calculation with a finite b-quark mass. In contrast, most of the above-mentioned calculations were done with a vanishing heavy-quark mass, with the justification that the quark mass is negligible at high transverse momentum (p_T). The ability to do NLO calculations with a finite heavy-quark mass for this class of processes was only recently demonstrated, for $Wb\bar{b}$, in Ref. [21] (and for $Zb\bar{b}$ in Ref. [16]). We will use this calculation, together with the NLO calculation of Wbj [22], to generate the NLO calculation of Wb, including the effect of the b-quark mass.

We discuss the details of the calculation in Section 2. We then present results in Section 3 and conclusions in Section 4.

2 Wb at NLO

The leading-order (LO) processes for the production of a W boson and one jet containing a b quark are shown in Fig. 1. In both cases there are two partons in the final state, but we require that only one of them (which contains a b quark) reside at high transverse momentum, with $p_{Tj} > 15$ GeV at the Fermilab Tevatron ($\sqrt{s} = 1.96$ TeV $p\bar{p}$) and $p_{Tj} > 25$ GeV at the CERN Large Hadron Collider (LHC, $\sqrt{s} = 14$ TeV pp). We also require this parton to lie within a pseudorapidity of $|\eta_j| < 2$ at the Tevatron and $|\eta_j| < 2.5$ at the LHC. Furthermore, we demand that two partons be separated by $|\Delta R| > 0.7$; if they are not, then their four-momenta are added and they are considered as occupying a single jet with this four-momentum. These requirements are made to crudely simulate the acceptance and resolution of the detectors. They are listed in Table 1, along with the parameters used in the calculations. In all calculations, the light quarks are summed over $q = u, d, s, c$, including CKM mixing.

The LO process shown in Fig. 1(b) contains a b quark in the initial state, and requires further discussion [26, 27]. To understand the usefulness of this approach, consider the

Table 1: Cuts used to simulate the acceptance and resolution of the detectors, and parameters used in the calculations.

Tevatron: $p_{Tj} > 15$ GeV	$|\eta_j| < 2$	
LHC: $\quad p_{Tj} > 25$ GeV	$|\eta_j| < 2.5$	
$|\Delta R_{b\bar{b}}| > 0.7$	$|\Delta R_{bj}| > 0.7$	

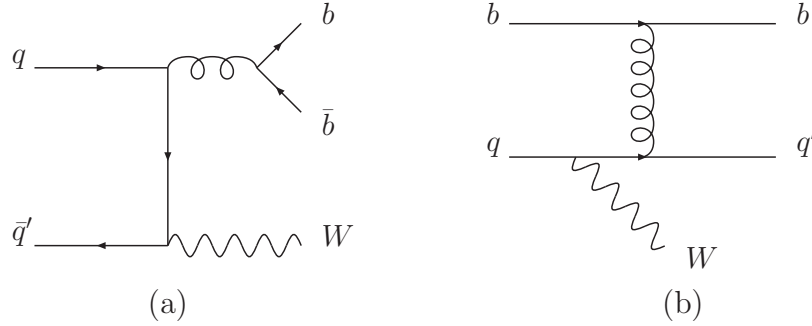|	
$M_W = 80.44$ GeV	$m_b = 4.7$ GeV
LO: CTEQ6L1	NLO: CTEQ6M [25]
$\mu_F = M_W$	$\mu_R = M_W$
$\alpha_S^{LO}(M_Z) = 0.130$	$\alpha_S^{LO}(M_W) = 0.132$
$\alpha_S^{NLO}(M_Z) = 0.118$	$\alpha_S^{NLO}(M_W) = 0.120$
$g^2 = 8M_W^2 G_F/\sqrt{2}$	$G_F = 1.16639 \times 10^{-5}$ GeV^{-2}
$V_{ud} = V_{cs} = 0.975$	$V_{us} = V_{cd} = 0.222$

(a)   (b)

Figure 1: Leading-order processes for the production of a W boson and one jet, which contains a b quark.

alternative approach, shown in Fig. 2 [28]. In that approach the b-quark mass is kept nonzero, so one obtains a finite result even when one of the b quarks is emitted at zero p_T. However, although the collinear singularity is regulated by the b mass, one obtains an enhancement factor of $\ln M_W/m_b$. Another power of this factor appears at each order of perturbation theory, degrading the convergence of the series. To ameliorate this, one sums this enhancement factor to all orders into a b distribution function, and uses this function in the LO calculation of Fig. 1(b). The other big advantage of this approach is that the LO process of Fig. 1(b) is simpler than that of Fig. 2, and hence a NLO calculation becomes tractable. This effectively allows to include a set of higher order corrections to the process of Fig. 2 that would appear only at NNLO in the fixed order calculation and will probably not be available for quite some time.

There are a variety of processes that must be calculated at NLO:

1. $q\bar{q}' \rightarrow Wb\bar{b}$ at tree level [Fig. 1(a)] and one loop ($m_b \neq 0$)

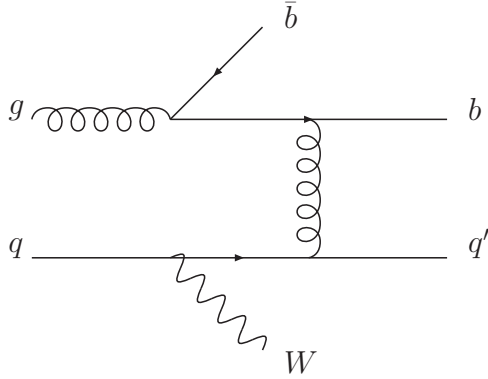2. $q\bar{q}' \rightarrow Wb\bar{b}g$ at tree level ($m_b \neq 0$)

Figure 2: An alternative way of calculating the process in Fig. 1(b).

3. $bq \to Wbq'$ at tree level [Fig. 1(b)] and one loop ($m_b = 0$)

4. $bq \to Wbq'g$ at tree level ($m_b = 0$)

5. $bg \to Wbq'\bar{q}$ at tree level ($m_b = 0$)

6. $gq \to Wb\bar{b}q'$ at tree level (Fig. 2) ($m_b \neq 0$)

Processes 1 and 2 are calculated with a non-zero b-quark mass, using the code developed in Ref. [21]. Processes 3–5, which involve an initial-state b quark, are calculated with $m_b = 0$, using the code developed in Ref. [22]. Process 6, calculated with a non-zero b-quark mass, can be taken from either code. We used this process to cross-check the two codes. We notice that the counterterm that subtracts from Process 6 the logarithmic terms already included in Process 3 has been added, in our calculation, to Processes 3-5, since it shares the same final state phase space configuration.

In the formalism that our calculation is based upon [26, 27], the b-quark mass is set to zero in any process in which the b quark appears in the initial state (Processes 3–5). This is not a limitation of the formalism, nor is it an approximation. In all other processes, where the b quark appears only in the final state, the b-quark mass is kept nonzero, although it is often a good approximation to set it to zero. For the calculation we are performing, it is essential to keep the b-quark mass nonzero. This is because we demand that only one b jet be at high p_T, and we do not restrict the other b quark. Thus there are regions of phase space where the $b\bar{b}$ invariant mass is not much greater than $2m_b$, in which case it is very inaccurate to neglect the b-quark mass [22]. This issue arises already at leading order, as evidenced by Fig. 3, where we show the $b\bar{b}$ invariant mass from Process 1 for the Wb exclusive cross section at the Tevatron for both $m_b = 0$ and $m_b = 4.7$ GeV (with $\Delta R_{jj} > 0.7$). We see that the cross section (the area under the curve) is very sensitive to the b-quark mass, even with the required separation of the two b quarks.

All NLO calculations are done in the $\overline{\text{MS}}$ scheme. When we refer to the NLO Processes 2, 4–6, it is understood that initial-state collinear singularities are subtracted in this scheme. For massless quarks, the collinear singularities are regulated dimensionally, while for massive b quarks (Processes 2 and 6) they are regulated using a finite b mass [22, 26, 27]. The calculation of Processes 3–6 was done using the Monte Carlo code MCFM [29, 30].
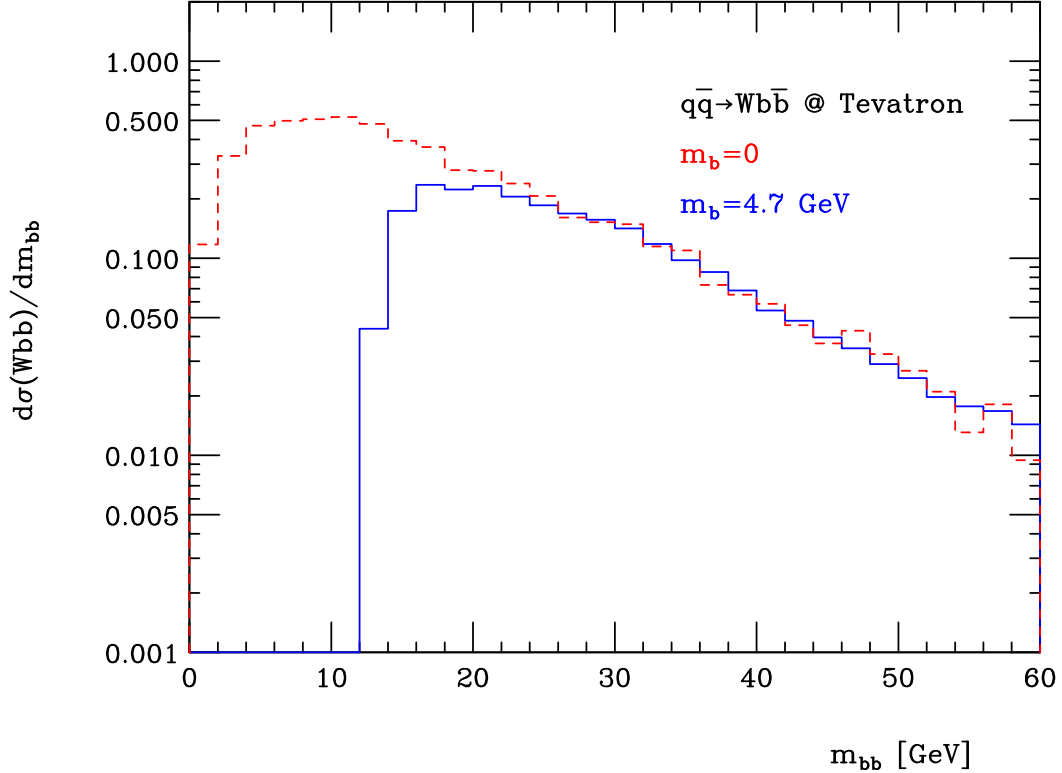
Figure 3: The differential cross section for W plus one b jet ($p_{Tj} > 15$ GeV, $|\eta_j| < 2$), *vs.* the invariant mass of the b quark and the other b quark (outside the fiducial region and separated by $\Delta R_{jj} > 0.7$), at the Fermilab Tevatron ($\sqrt{S} = 1.96$ TeV $p\bar{p}$). Only the contribution from the LO subprocess $q\bar{q} \to W b\bar{b}$ is shown. The (solid, blue) curve includes the b quark mass, while the (dashed, red) curve does not.

3   Results

In Table 2, we give the exclusive cross section for $W + 1$ jet, where the jet contains a b quark, and there are no other jets present within the acceptance (listed in Table 1). We list the cross section for the case where there is only one b in the jet (denoted Wb), and when there are two b's in the jet (denoted $W(b\bar{b})$). The tagging probability for a jet with two b's differs from that of a jet with one b [31]. We notice that in the $W(b\bar{b})$ case the two b quarks can be collinear and give origin to large logarithms of the form $\ln(p_T^b/m_b)$. Our results do not contain a resummation of these logarithms and are therefore subject to some degree of uncertainty. We could have rejected the $W(b\bar{b})$ configuration in our $W + b$-jet NLO results or used a different jet algorithm as suggested, for instance, in Ref. [32]. We prefer to keep it and quote it separately in order to make it available to different kinds of experimental analyses. Table 2 gives both the LO cross section (in square brackets)[1] and the NLO cross section. The first number given is from Processes 1–2; the second from Processes 3–6; and

---

[1]The contribution from Process 1 to the Wb cross section at the Tevatron corresponds, at LO, to the area under the (solid, blue) curve in Fig. 3.

the third is their sum. In the case of Wb we also quote, in parenthesis, the contribution of Process 6 by itself. Indeed Process 6 is part of both the fixed order $(1+2+6)$ and resummed $(3+4+5+6)$ calculations[2] and results could be quoted grouping Processes either way. In order to assess the impact of resumming initial state collinear logarithms, however, one needs to compare the sum of Processes 1,2, and 6 to the sum of process 3, 4, and 5. This can be easily deduced from our Tables knowing Process 6 independently. In the case of $W(b\bar{b})$, only Process 1 contributes at LO, and only Processes 1–2,6 at NLO. Thus we do not need to quote Process 6 separately. The NLO results correspond to a pure fixed order calculation. We see that at the Tevatron, Processes 1–2 make a much larger contribution to Wb than Processes 3–6, while at the LHC the two sets of processes make comparable contributions. This mirrors the results for the Wbj final state [22], first noted in Ref. [28]. The fixed order calculation (Processes $1+2+6$) dominates at both the Tevatron and the LHC, but the corrections included in Processes 3+4+5 are as much as 25% at the LHC and therefore very relevant. We also notice that for both Wb and $W(b\bar{b})$ Processes 1–2 dominate at the Tevatron, while at the LHC Process 6 is nearly half the size of Processes 1–2. Therefore it is very important to include higher order corrections to this process, as it is achieved by adding to the fixed order result Process 3, 4 and 5 (see discussion in Sec. 2). Finally, we notice that for $W(b\bar{b})$, the NLO cross section is significantly larger than the LO cross section, while the NLO correction is modest for Wb.

Also given in Table 2 is the exclusive cross section for Wj ($j = u, d, s, c, g$), both at LO and NLO [33, 34]. These numbers are useful to compute the fraction of $W + 1j$ events in which the jet contains a b quark. This fraction is around 0.7% at the Tevatron and 0.8% at the LHC.

We give in Table 3 the inclusive cross sections for $W + 1j + X$, where the jet contains a b quark, and where there may be other jets present (up to two additional jets at NLO). The relative importance of Processes 3–6 is significantly increased compared with the exclusive cross sections, especially at the LHC, due in particular to Process 6. This is expected since Process 6 is more effectively cut in the exclusive cross section where the NLO cross section is required to have the same number of jets as the LO cross section. The fixed order cross section (Processes 1+2+6) dominates at both the Tevatron and LHC, but corrections coming from Processes 3+4+5 are large and of the order of 50% at the LHC. Moreover, given the relevance of Process 6, having included part of the NLO corrections to Process 6 by calculating Process 3 at NLO in QCD increases the stability and therefore the validity of the theoretical prediction. The NLO cross sections are also increased by a larger factor than in the exclusive cross sections. The fraction of $W + 1j + X$ events in which the jet contains a b quark is around 0.9% at the Tevatron and 1.2% at the LHC.

---

[2]As explained in Section 2, Process 6 is the same in both the resummed and fixed order calculations, i.e. it does not include any counterterm to subtract the logarithmic terms that have been resummed in Process 3. Such counterterm has been included with Process 3 since it shares the same final state phase space.

Table 2: Exclusive cross sections (pb) for W boson plus one jet, which contains at least one b quark, at the Tevatron ($\sqrt{s} = 1.96$ TeV $p\bar{p}$) and LHC ($\sqrt{s} = 14$ TeV pp). No branching ratios or tagging efficiencies are included. The labels on the columns have the following meaning: Wb = exactly one jet, which contains a b quark; $W(b\bar{b})$ = exactly one jet, which contains two b quarks; Wj = exactly one jet, including both light quarks (u, d, s, c) and gluons. Both the leading-order (in square brackets) and next-to-leading-order cross sections are given. The first number given is from Processes 1–2; the second number is from Processes 3–6 (with Process 6 given separately in parenthesis); and the third number is their sum.

	Exclusive cross sections (pb)	
Collider	Wb	$W(bb)$
TeV $W^+(= W^-)$	[5.28+0.75=6.03] 8.02+0.62(-0.05)=8.64	[2.66] 3.73-0.02=3.71
LHC W^+	[30.2+54.3=84.5] 40.0+48.4(22.6)=88.4	[17.6] 22.7+11.7=34.4
LHC W^-	[21.6+31.4=53.0] 29.8+29.4(12.6)=59.2	[12.9] 17.2+6.5=23.7
	Wj	
TeV $W^+(= W^-)$	[1410] 1790	
LHC W^+	[14240] 15810	
LHC W^-	[11040] 12040	

We estimate the theoretical uncertainty in the exclusive and inclusive LO and NLO cross sections by varying the renormalization (μ_R) and factorization (μ_F) scales independently. We vary μ_R in the $(0.5-2)M_W$ range while keeping μ_F fixed at its central value, $\mu_F = M_W$. Similarly we vary μ_F in the $(0.5-2)M_W$ range keeping $\mu_R = M_W$. The results are illustrated in Figs. 4 and 5, where the plots on the l.h.s. correspond to W production with a b jet (Wb) while the plots on the r.h.s. correspond to W production with a double-b jet ($W(b\bar{b})$). The upper plots refer to $W^+b/W^+(b\bar{b}) = W^-b/W^-(b\bar{b})$ production at the Tevatron, the middle plots to $W^+b/W^+(b\bar{b})$ production at the LHC, and the lower plots to $W^-b/W^-(b\bar{b})$ production at the LHC. The cross sections in Figs. 4 and 5 have been normalized to their $\mu_R = \mu_F = M_W$ value. The horizontal axis represents the variation of either μ_R or μ_F, depending on the curve (see figure captions), normalized to the central value $\mu_0 = M_W$. In Tables 4 and 5 we quantitatively give the variation with μ_R and μ_F as (asymmetric) uncertainties on the central value, corresponding to the choice $\mu_R = \mu_F = M_W$ used to obtain the results of Tables 2 and 3. We have not included in the theoretical uncertainties reported in this paper the uncertainty coming from the parton distribution functions.

From Figs. 4 (and 5 and Tables 4 and 5) we see that the theoretical uncertainty due to the dependence on the renormalization scale is larger than the corresponding uncertainty from the factorization-scale dependence. The decrease in the factorization-scale dependence in going from LO to NLO is mild, while the decrease in the renormalization-scale dependence is significant. An exception is the inclusive $W(b\bar{b})$ cross-sections at the LHC, where the renormalization-scale dependence slightly increases at NLO. Even in the exclusive case, the improvement in the renormalization-scale dependence in going from LO to NLO for $W(b\bar{b})$ is mild at the LHC. These exceptions can be explained by the fact that only Processes 1–2,6 contribute to $W(b\bar{b})$ production at NLO and, among those, Process 6 opens a new initial

Table 3: Inclusive cross sections (pb) for W boson plus one jet, which contains at least one b quark, at the Tevatron ($\sqrt{s} = 1.96$ TeV $p\bar{p}$) and LHC ($\sqrt{s} = 14$ TeV pp). No branching ratios or tagging efficiencies are included. The labels on the columns have the following meaning: $Wb+X$ = one or more jets, at least one of which contains a b quark; $W(b\bar{b})+X$ = one or more jets, one of which contains two b quarks; $Wj+X$ = one or more jets, including both light quarks (u, d, s, c) and gluons. Both the leading-order (in square brackets) and next-to-leading-order cross sections are given. The first number given is from Processes 1–2; the second number is from Processes 3–6 red (with Process 6 given separately in parenthesis); and the third number is their sum.

	Inclusive cross sections (pb)	
Collider	$Wb+X$	$W(b\bar{b})+X$
TeV $W^+(=W^-)$	[7.56+1.81=9.37] 11.77+2.40(0.77)=14.17	[2.66] 4.17+0.39=4.56
LHC W^+	[39.3+106.0=145.3] 53.6+136.1(68.9)=189.7	[17.6] 25.1+35.9=61.0
LHC W^-	[27.9+67.0=94.9] 39.3+88.2(44.6)=127.5	[12.9] 18.9+23.6=42.5
	$Wj+X$	
TeV $W^+(=W^-)$	[1410] 2030	
LHC W^+	[14240] 20000	
LHC W^-	[11040] 15220	

state, namely qg, and is effectively a LO process. The effect is larger at the LHC because, due to the large gluon density, the qg channel is more relevant. The effect is also larger for inclusive rather than exclusive cross sections because the exclusive final state suppresses the contribution of Process 6 (which is a $2 \rightarrow 4$ process), as evidenced by the numerical results in Tables 2 and 3.

In Figs. 6–9 we show the differential cross sections with respect to the transverse momentum of the b jet and of the W boson, for W^+b inclusive/exclusive and $W^+(b\bar{b})$ inclusive/exclusive production. If there is more than one b jet in the final state, the p_T of the highest-p_T b jet is chosen. We do not show distributions for W^-b and $W^-(b\bar{b})$ production at the LHC, since they resemble the ones for W^+b and $W^+(b\bar{b})$ production at the LHC illustrated here. For all final states, the NLO QCD corrections modify the shape of both the b-jet and W-boson transverse momentum distributions.

4 Conclusions

In this paper we report on a NLO calculation of the production of a W boson with one b jet. We present both inclusive and exclusive cross sections, as well as cross sections where the jet contains one or two b quarks. We show that it is essential to keep the b-quark mass finite throughout the calculation, and we are able to overcome this technical hurdle. The calculation is performed by combining two previous NLO calculations of $Wb\bar{b}$ [21] and Wbj [22], taking care to treat their overlap consistently. The calculation that we present thus represents the state of the art prediction for W plus one b jet production at NLO in QCD.

Table 4: Exclusive cross sections (pb) for W boson plus one jet, which contains at least one b quark, with the theoretical uncertainty due to renormalization (first uncertainty) and factorization (second uncertainty) scale dependence. The uncertainty due to the renormalization scale (μ_R) dependence is estimated by varying μ_R by a factor of two with respect to its central value $\mu_R = M_W$, while keeping the factorization scale (μ_F) fixed at its central value $\mu_F = M_W$. The uncertainty due to the factorization scale is estimated analogously, i.e. varying μ_F by a factor of two about its central value $\mu_F = M_W$, while keeping μ_R fixed at $\mu_R = M_W$. The central values are extracted from Table 2. The labeling of columns and rows are as described in the caption of Table 2. Results within brackets are LO, results with no brackets are NLO.

	Exclusive cross sections (pb)	
Collider	Wb	$W(bb)$
TeV $W^+(=W^-)$	$[6.03\times(1^{+0.27+0.02}_{-0.19-0.03})]$ $8.64\times(1^{+0.13+0.004}_{-0.12-0.003})$	$[2.66\times(1^{+0.27+0.04}_{-0.19-0.04})]$ $3.71\times(1^{0.12+0.01}_{-0.11-0.01})$
LHC W^+	$[84.5\times(1^{+0.27+0.11}_{-0.19-0.14})]$ $88.4\times(1^{+0.11+0.08}_{-0.11-0.10})$	$[17.6\times(1^{+0.27+0.09}_{-0.19-0.10})]$ $34.4\times(1^{+0.23+0.03}_{-0.16-0.04})$
LHC W^-	$[53.0\times(1^{+0.27+0.12}_{-0.19-0.14})]$ $59.2\times(1^{+0.12+0.08}_{-0.11-0.10}$	$[12.9\times(1^{+0.27+0.09}_{-0.19-0.11})]$ $23.7\times(1^{+0.21+0.03}_{-0.15-0.04})$

These calculations can be compared with the large amount of data on W plus b jets already gathered at the Tevatron, and soon to be produced at the LHC. They can also be compared with the inclusive samples obtained by merging matrix-element calculations with parton showers.
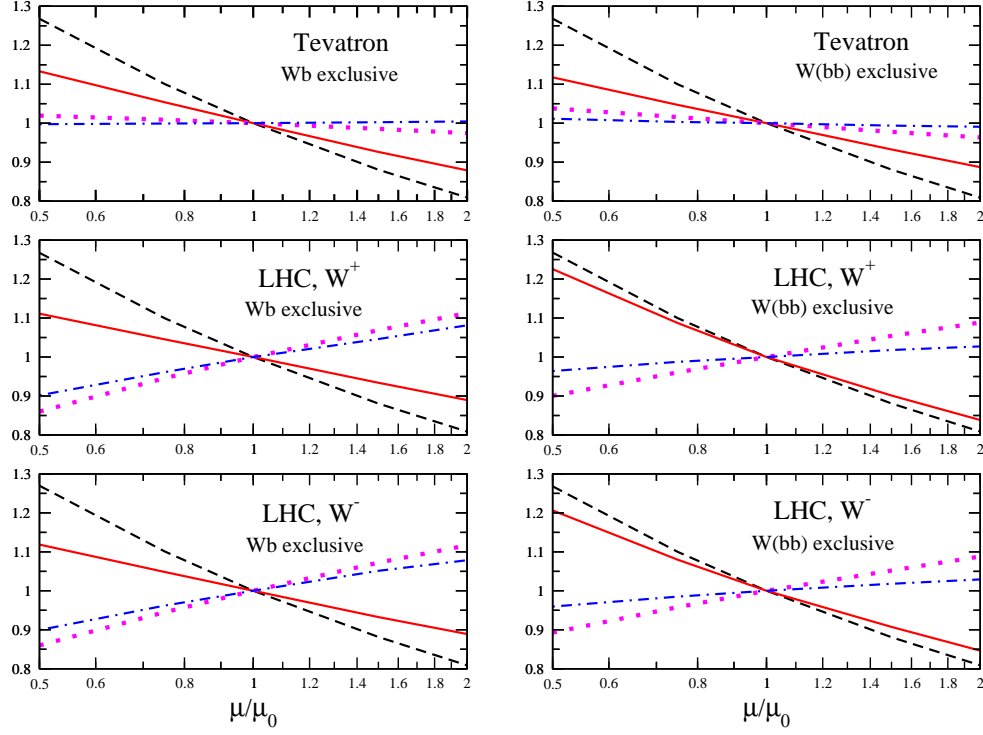
Acknowledgments

Figure 4: Renormalization- and factorization-scale dependence of Wb (l.h.s.) and $W(b\bar{b})$ (r.h.s.) exclusive production. The upper plots correspond to both $W^+b/W^+(b\bar{b})$ and $W^-b/W^-(b\bar{b})$ production at the Tevatron. The middle plots correspond to $W^+b/W^+(b\bar{b})$ production at the LHC and the lower plots correspond to $W^-b/W^-(b\bar{b})$ production at the LHC. The black dashed (LO) and red solid (NLO) curves represent the dependence on the renormalization scale (μ_R) when μ_R is varied with respect to its central value $\mu_0 = M_W$, while the factorization scale (μ_F) is fixed at $\mu_F = M_W$. In a similar way, the magenta dotted (LO) and blue dot-dashed (NLO) curves represent the dependence on μ_F when μ_F is varied with respect to its central value $\mu_0 = M_W$, while μ_R is fixed at $\mu_R = M_W$. The cross sections have been normalized to their $\mu_R = \mu_F = M_W$ value.
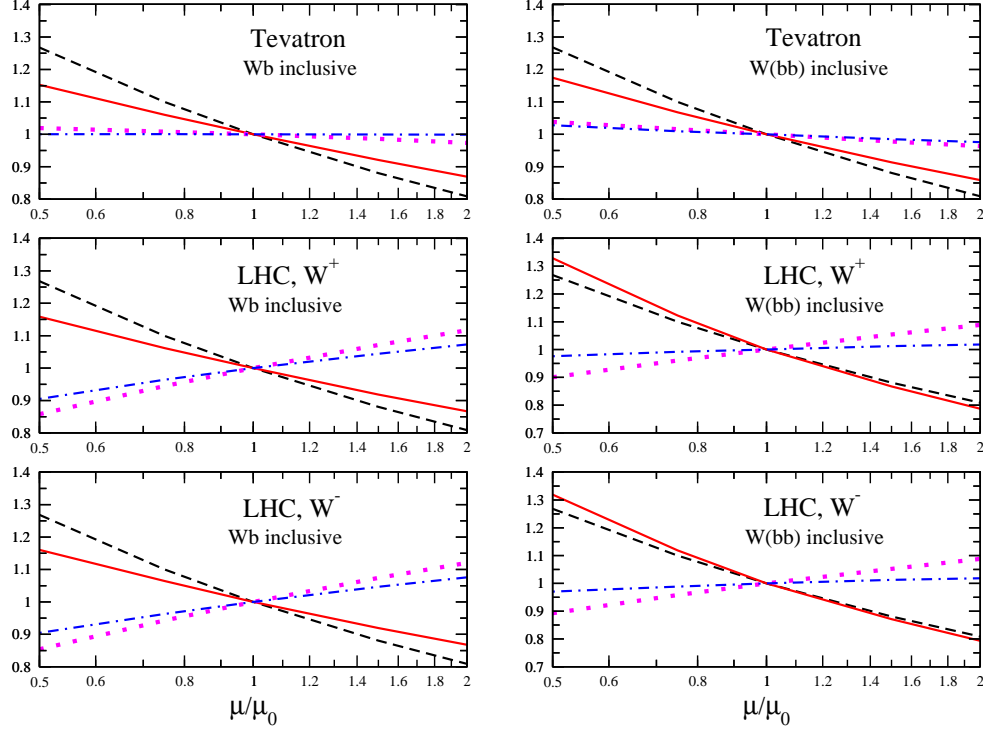
Figure 5: Renormalization- and factorization-scale dependence of Wb (l.h.s.) and $W(b\bar{b})$ (r.h.s.) inclusive production. The upper plots correspond to both $W^+b/W^+(b\bar{b})$ and $W^-b/W^-(b\bar{b})$ production at the Tevatron. The middle plots correspond to $W^+b/W^+(b\bar{b})$ production at the LHC and the lower plots correspond to $W^-b/W^-(b\bar{b})$ production at the LHC. The black dashed (LO) and red solid (NLO) curves represent the dependence on the renormalization scale (μ_R) when μ_R is varied with respect to its central value $\mu_0 = M_W$, while the factorization scale (μ_F) is fixed at $\mu_F = M_W$. In a similar way, the magenta dotted (LO) and blue dot-dashed (NLO) curves represent the dependence on μ_F when μ_F is varied with respect to its central value $\mu_0 = M_W$, while μ_R is fixed at $\mu_R = M_W$. The cross sections have been normalized to their $\mu_R = \mu_F = M_W$ value.

10

Table 5: Inclusive cross sections (pb) for W boson plus one jet, which contains at least one b quark, with the theoretical uncertainty due to renormalization (first uncertainty) and factorization (second uncertainty) scale dependence. The uncertainty due to the renormalization scale (μ_R) dependence is estimated by varying μ_R by a factor of two with respect to its central value $\mu_R = M_W$, while keeping the factorization scale (μ_F) fixed at its central value $\mu_F = M_W$. The uncertainty due to the factorization scale is estimated analogously, i.e. varying μ_F by a factor of two about its central value $\mu_F = M_W$, while keeping μ_R fixed at $\mu_R = M_W$. The central values are extracted from Table 3. The labeling of columns and rows are as described in the caption of Table 3. Results within brackets are LO, results with no brackets are NLO.

Collider	Inclusive cross sections (pb)	
	Wb	$W(bb)$
TeV $W^+(=W^-)$	$[9.37\times(1^{+0.27+0.02}_{-0.19-0.03})]\ 14.17\times(1^{+0.15+0.0002}_{-0.13-0.001})$	$[2.66\times(1^{+0.27+0.04}_{-0.19-0.04})]\ 4.56\times(1^{+0.17+0.03}_{-0.14-0.02})$
LHC W^+	$[145.3\times(1^{+0.27+0.12}_{-0.19-0.14})]\ 189.7\times(1^{+0.16+0.07}_{-0.13-0.10})$	$[17.6\times(1^{+0.27+0.09}_{-0.19-0.10})]\ 61.0\times(1^{+0.33+0.02}_{-0.21-0.02})$
LHC W^-	$[94.9\times(1^{+0.27+0.12}_{-0.19-0.15})]\ 127.5\times(1^{+0.16+0.08}_{-0.13-0.10})$	$[12.9\times(1^{+0.27+0.09}_{-0.19-0.11})]\ 42.5\times(1^{+0.32+0.02}_{-0.21-0.03})$

References

[1] F. Abe *et al.* [CDF Collaboration], Phys. Rev. Lett. **74**, 2626 (1995) [arXiv:hep-ex/9503002].

[2] S. Abachi *et al.* [D0 Collaboration], Phys. Rev. Lett. **74**, 2632 (1995) [arXiv:hep-ex/9503003].

[3] V. M. Abazov *et al.* [D0 Collaboration], Phys. Rev. Lett. **98**, 181802 (2007) [arXiv:hep-ex/0612052].

[4] V. M. Abazov *et al.* [D0 Collaboration], Phys. Rev. D **78**, 012005 (2008) [arXiv:0803.0739 [hep-ex]].

[5] D. Acosta *et al.* [CDF Collaboration], Phys. Rev. D **71**, 012005 (2005) [arXiv:hep-ex/0410058].

[6] http://www-cdf.fnal.gov/physics/new/top/public_singletop.html

[7] T. Aaltonen *et al.* [CDF Collaboration], Phys. Rev. Lett. **100**, 041801 (2008) [arXiv:0710.4363 [hep-ex]].

[8] T. Aaltonen *et al.* [CDF Collaboration], arXiv:0803.3493 [hep-ex].

[9] V. M. Abazov *et al.* [D0 Collaboration], Phys. Lett. B **663**, 26 (2008) [arXiv:0712.0598 [hep-ex]].

[10] V. M. Abazov *et al.* [D0 Collaboration], Phys. Lett. B **655**, 209 (2007) [arXiv:0704.2000 [hep-ex]].
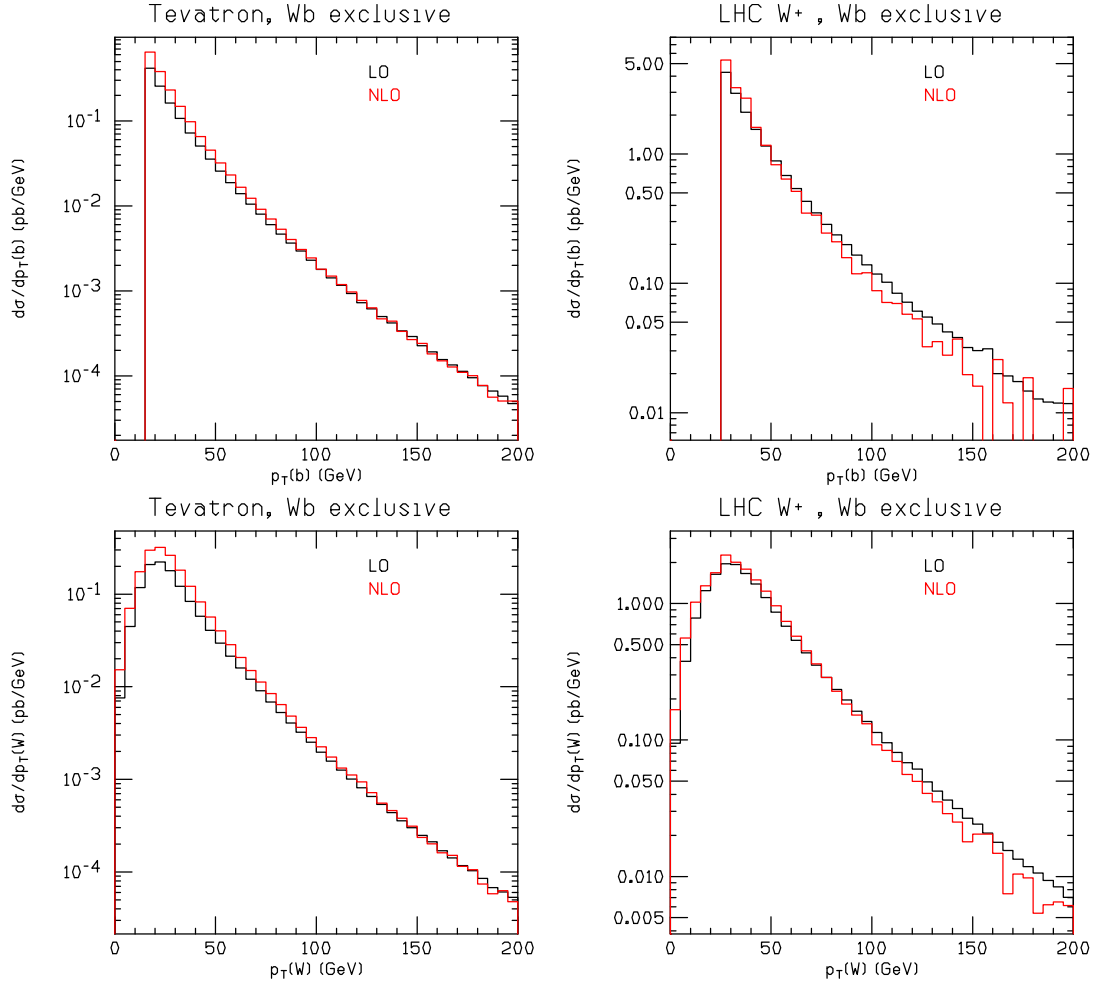
Figure 6: $p_T(b)$ (upper plots) and $p_T(W)$ (lower plots) distributions for W^+b *exclusive* production, at the Tevatron (l.h.s. plots) and at the LHC (r.h.s. plots).
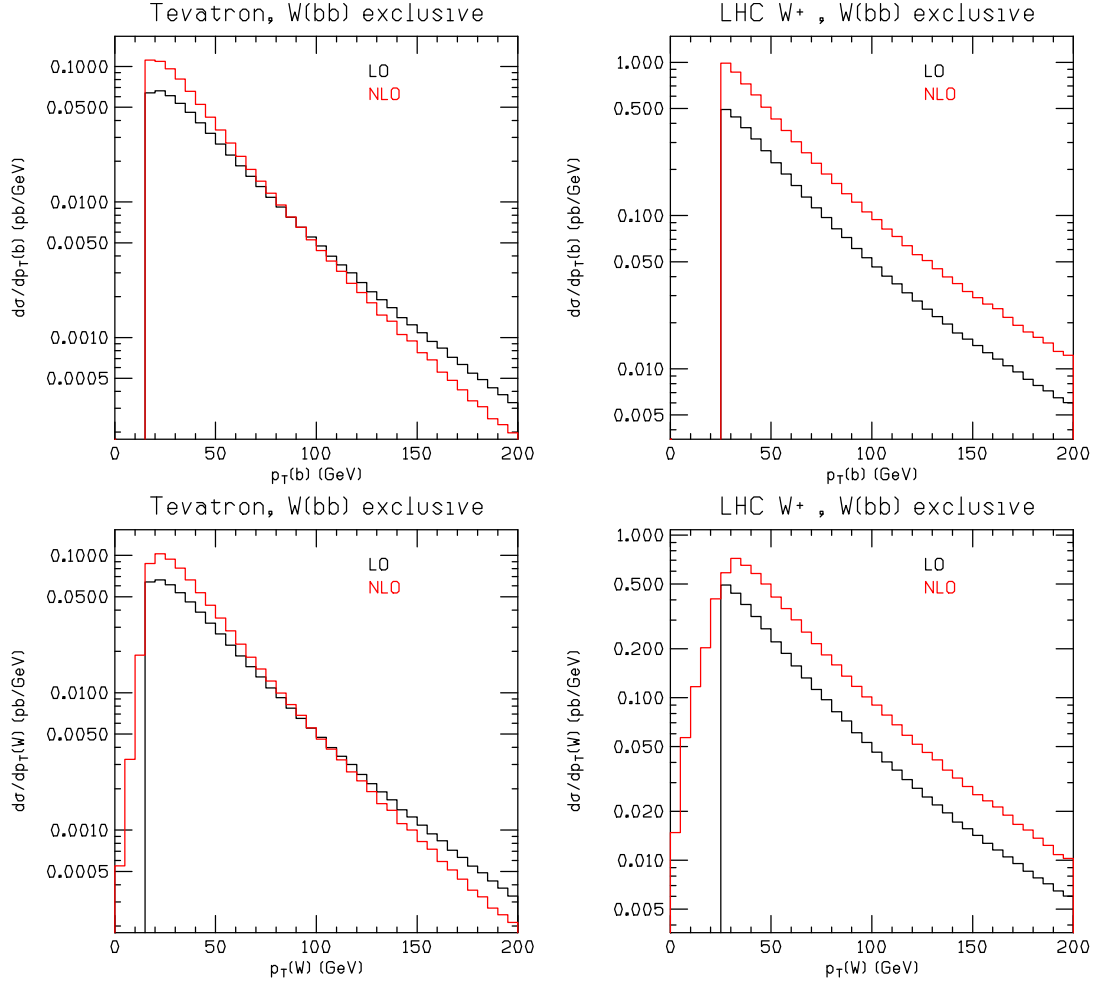
Figure 7: $p_T(b)$ (upper plots) and $p_T(W)$ (lower plots) distributions for $W^+(b\bar{b})$ *exclusive* production, at the Tevatron (l.h.s. plots) and at the LHC (r.h.s. plots).
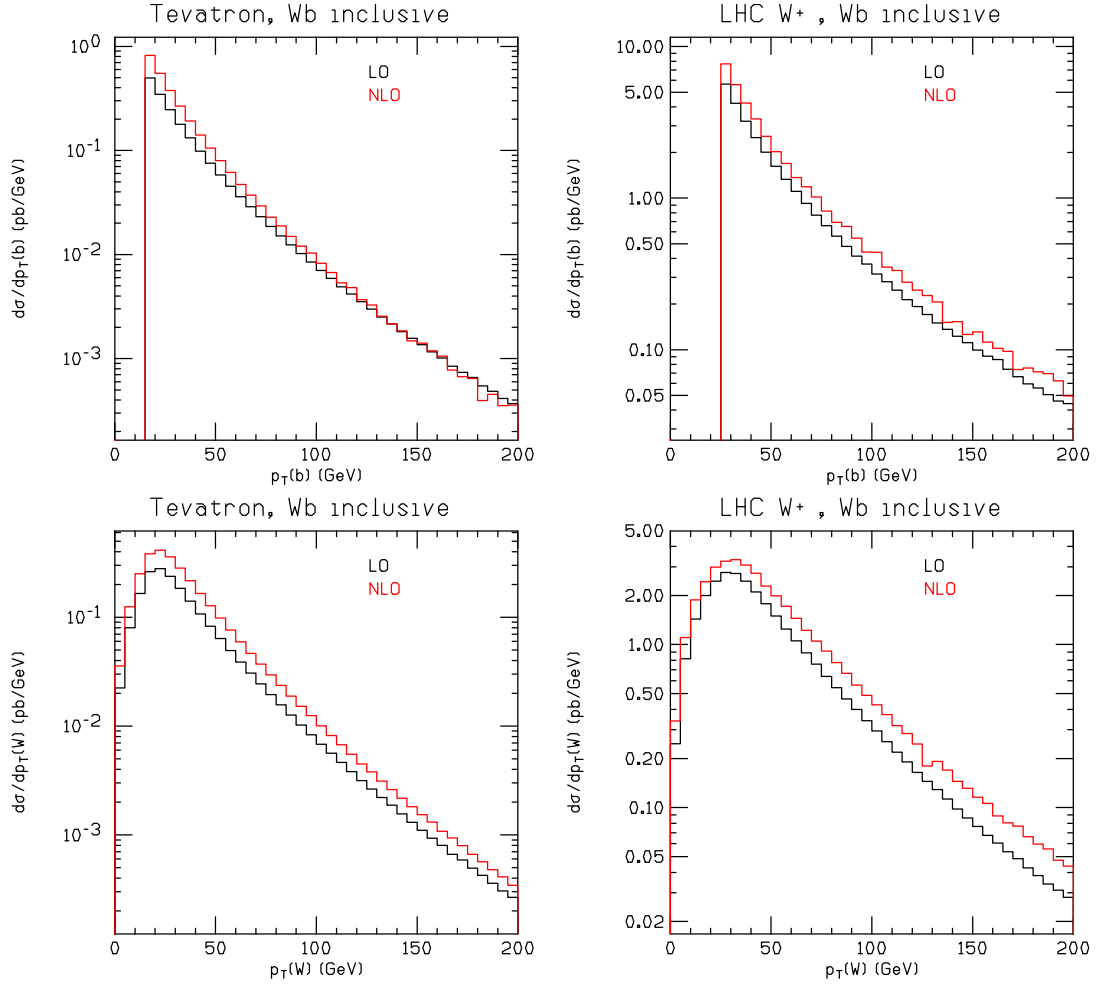
13

Figure 8: $p_T(b)$ (upper plots) and $p_T(W)$ (lower plots) distributions for W^+b *inclusive* production, at the Tevatron (l.h.s. plots) and at the LHC (r.h.s. plots).
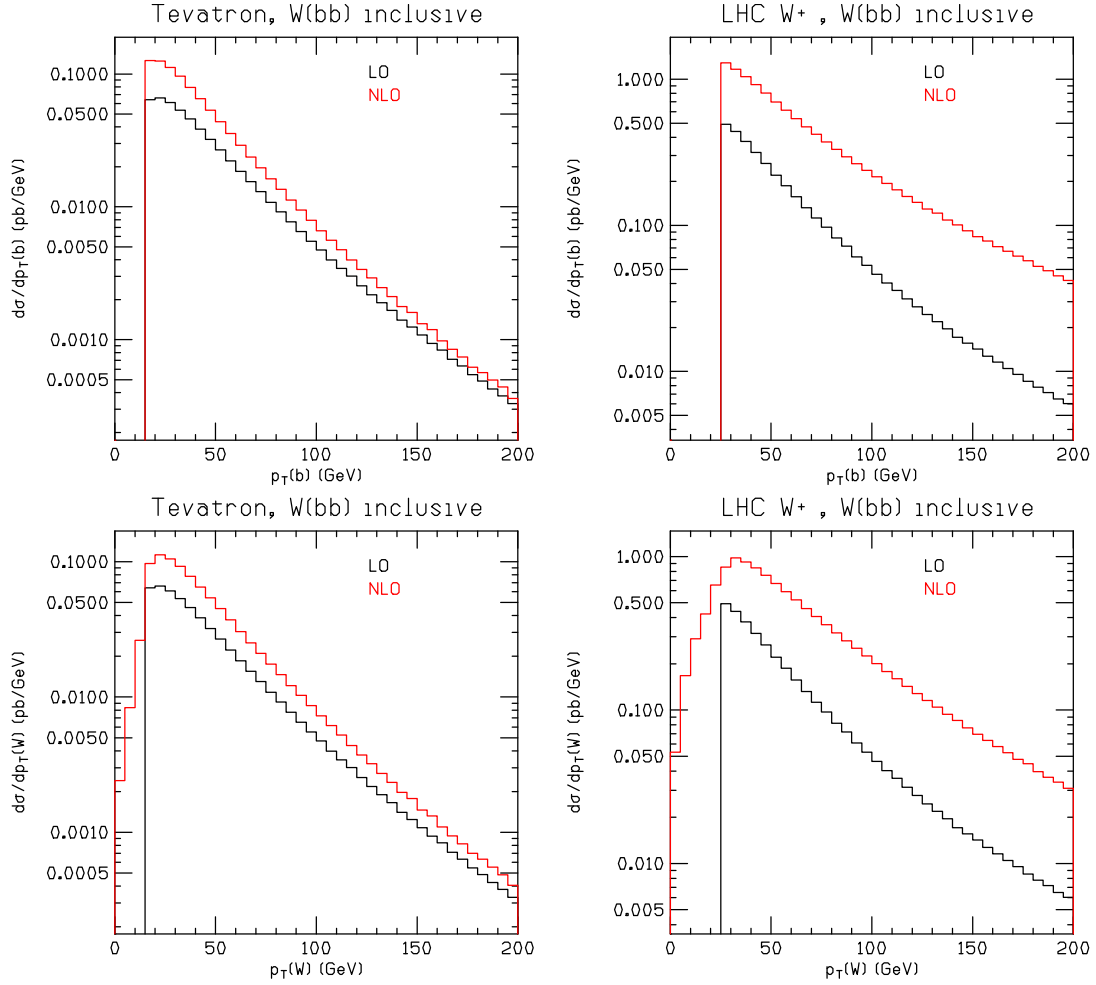
14

Figure 9: $p_T(b)$ (upper plots) and $p_T(W)$ (lower plots) distributions for $W^+(b\bar{b})$ *inclusive* production, at the Tevatron (l.h.s. plots) and at the LHC (r.h.s. plots).

15

[11] T. Aaltonen *et al.* [CDF Collaboration], Phys. Rev. Lett. **100**, 211801 (2008) [arXiv:0802.0432 [hep-ex]].

[12] Z. Bern, L. J. Dixon, D. A. Kosower and S. Weinzierl, Nucl. Phys. B **489**, 3 (1997) [arXiv:hep-ph/9610370].

[13] Z. Bern, L. J. Dixon and D. A. Kosower, Nucl. Phys. B **513**, 3 (1998) [arXiv:hep-ph/9708239].

[14] J. Campbell, R. K. Ellis, F. Maltoni and S. Willenbrock, Phys. Rev. D **69**, 074021 (2004) [arXiv:hep-ph/0312024].

[15] J. M. Campbell and R. K. Ellis, Phys. Rev. D **62**, 114012 (2000) [arXiv:hep-ph/0006304].

[16] F. Febres Cordero, L. Reina and D. Wackeroth, arXiv:0806.0808 [hep-ph].

[17] J. Campbell, R. K. Ellis, F. Maltoni and S. Willenbrock, Phys. Rev. D **73**, 054007 (2006) [arXiv:hep-ph/0510362].

[18] W. T. Giele, S. Keller and E. Laenen, Phys. Lett. B **372**, 141 (1996) [arXiv:hep-ph/9511449].

[19] J. Campbell, R. K. Ellis and R. Mahbubani, in preparation.

[20] R. K. Ellis and S. Veseli, Phys. Rev. D **60**, 011501 (1999) [arXiv:hep-ph/9810489].

[21] F. Febres Cordero, L. Reina and D. Wackeroth, Phys. Rev. D **74**, 034007 (2006) [arXiv:hep-ph/0606102].

[22] J. Campbell, R. K. Ellis, F. Maltoni and S. Willenbrock, Phys. Rev. D **75**, 054015 (2007) [arXiv:hep-ph/0611348].

[23] M. L. Mangano, M. Moretti, F. Piccinini, R. Pittau and A. D. Polosa, JHEP **0307**, 001 (2003) [arXiv:hep-ph/0206293].

[24] F. Maltoni and T. Stelzer, JHEP **0302**, 027 (2003) [arXiv:hep-ph/0208156].

[25] J. Pumplin, D. R. Stump, J. Huston, H. L. Lai, P. Nadolsky and W. K. Tung, JHEP **0207**, 012 (2002) [arXiv:hep-ph/0201195].

[26] M. A. G. Aivazis, J. C. Collins, F. I. Olness and W. K. Tung, Phys. Rev. D **50**, 3102 (1994) [arXiv:hep-ph/9312319].

[27] J. C. Collins, Phys. Rev. D **58**, 094002 (1998) [arXiv:hep-ph/9806259].

[28] M. L. Mangano, M. Moretti and R. Pittau, Nucl. Phys. B **632**, 343 (2002) [arXiv:hep-ph/0108069].

[29] R. K. Ellis *et al.* [QCD Tools Working Group], arXiv:hep-ph/0011122.

[30] J. Campbell and R. K. Ellis, MCFM - Monte Carlo for FeMtobarn processes, http://mcfm.fnal.gov/.

[31] D. Acosta *et al.* [CDF Collaboration], Phys. Rev. D **71**, 092001 (2005) [arXiv:hep-ex/0412006].

[32] A. Banfi, G. P. Salam and G. Zanderighi, JHEP **0707**, 026 (2007) [arXiv:0704.2999 [hep-ph]].

[33] W. T. Giele, E. W. N. Glover and D. A. Kosower, Nucl. Phys. B **403**, 633 (1993) [arXiv:hep-ph/9302225].

[34] J. Campbell and R. K. Ellis, Phys. Rev. D **65**, 113007 (2002) [arXiv:hep-ph/0202176].